

11-15-1988

# Transport Critical Current and Magnetization Measurements of Melt-Processed $\text{YBa}_2\text{Cu}_3\text{O}_{7-x}$

A. H. Hermann

Z. Z. Sheng

W. Kiehl

D. Marsh

A. Elali

*See next page for additional authors*

Follow this and additional works at: [https://engagedscholarship.csuohio.edu/sciphysics\\_facpub](https://engagedscholarship.csuohio.edu/sciphysics_facpub)

 Part of the [Physics Commons](#)

**How does access to this work benefit you? Let us know!**

## *Publisher's Statement*

Copyright 1988 American Institute of Physics. This article may be downloaded for personal use only. Any other use requires prior permission of the author and the American Institute of Physics. The following article appeared in *Journal of Applied Physics* 64 (1988): 5050-5055 and may be found at <http://link.aip.org/link/doi/10.1063/1.342459>.

## Original Citation

Hermann, A. H., Z. Z. Sheng, W. Kiehl, D. Marsh, A. Elali, Paul D. Hambourger, C. Almasan, J. Estrada, and T. Datta. "Transport Critical Current and Magnetization Measurements of Melt-Processed  $\text{YBa}_2\text{Cu}_3\text{O}_{7-x}$ ." *Journal of Applied Physics* 64 (1988): 5050-5055.

## Repository Citation

Hermann, A. H.; Sheng, Z. Z.; Kiehl, W.; Marsh, D.; Elali, A.; Hambourger, Paul D.; Almasan, C.; Estrada, J.; and Datta, T., "Transport Critical Current and Magnetization Measurements of Melt-Processed  $\text{YBa}_2\text{Cu}_3\text{O}_{7-x}$ " (1988). *Physics Faculty Publications*. 94.  
[https://engagedscholarship.csuohio.edu/sciphysics\\_facpub/94](https://engagedscholarship.csuohio.edu/sciphysics_facpub/94)

This Article is brought to you for free and open access by the Physics Department at EngagedScholarship@CSU. It has been accepted for inclusion in Physics Faculty Publications by an authorized administrator of EngagedScholarship@CSU. For more information, please contact [library.es@csuohio.edu](mailto:library.es@csuohio.edu).

---

**Authors**

A. H. Hermann, Z. Z. Sheng, W. Kiehl, D. Marsh, A. Elali, Paul D. Hamburger, C. Almasan, J. Estrada, and T. Datta

# Transport critical current and magnetization measurements of melt-processed $\text{YBa}_2\text{Cu}_3\text{O}_{7-x}$

A. H. Hermann, Z. Z. Sheng, W. Kiehl, D. Marsh, and A. El Ali  
*Department of Physics, University of Arkansas, Fayetteville, Arkansas 72701*

P. D. Hambourger  
*Department of Physics, Cleveland State University, Cleveland, Ohio 44115*

C. Aimasan, J. Estrada, and T. Datta  
*Department of Physics, University of South Carolina, Columbia, South Carolina 29208*

(Received 7 June 1988; accepted for publication 8 August 1988)

We report magnetic field dependence of the transport critical current and dc magnetic susceptibility measurements on  $\text{YBa}_2\text{Cu}_3\text{O}_{7-x}$  superconductors formed by melt-solid reactions at 950 °C between Ba-Cu-O (or Tb-Ba-Cu-O) and solid nonstoichiometric Y-Ba-Cu-oxide. Four-probe dc critical current measurements at 77, 64, and 4.2 K show strong depression of the critical current density with increasing magnetic field in agreement with a model of weakly linked superconducting regions. Diamagnetic shielding and Meissner flux expulsion measurements in the temperature range 10–300 K show about one third volume fraction of perfect superconductivity. Both shielding and flux expulsion were observed to be approximately temperature independent below 60 K indicating strong coupling between the grains throughout the entire volume below this temperature.

## I. INTRODUCTION

High-quality high-temperature superconductors based on melt-solid reactions at 950 °C between molten Ba-Cu-oxide (or Tb-Ba-Cu-oxides) and solid nonstoichiometric rare-earth-Ba-Cu-quaternary oxides, rare-earth-Ba-Cu-ternary oxides, rare-earth-Cu-ternary oxides or rare-earth-Ba-ternary oxides, and even rare-earth binary oxides have been reported.<sup>1,2</sup> The melt processed superconductors take on the rare-earth-Ba-Cu-O (123) stoichiometry with distorted perovskite structure. Their critical temperatures all exceed 90 K. We report here magnetic field dependence of four-probe critical current measurements at 77, 64, and 4.2 K and static magnetic susceptibility measurements for the range of 10–300 K.

## II. EXPERIMENT

Samples were prepared as previously described.<sup>1,2</sup> Appropriate amounts of  $\text{BaCO}_3$  and  $\text{CuO}$  were mixed and ground in an agate mortar and heated in air at 900 °C for 12 h to obtain the melting starting material with nominal composition of  $\text{BaCu}_3\text{O}_4$  or  $\text{Ba}_2\text{Cu}_3\text{O}_5$ . In each case the heated mixture was reground and pressed into pellets. In the case of the Tb starting compounds, appropriate mixtures of  $\text{Tb}_4\text{O}_7$ ,  $\text{BaCO}_3$ , and  $\text{CuO}$  powders were prepared similarly. The solid nonmelting starting materials were prepared from  $\text{Y}_2\text{O}_3$ ,  $\text{BaCO}_3$ , and  $\text{CuO}$  and were mixed, ground, and heated in air at 950 °C for 12 h to obtain compounds with nominal compositions  $\text{Y}_{1.2}\text{Ba}_{0.8}\text{CuO}_{3.6+x}$  or  $\text{YBaO}_{2.5}$  or  $\text{YCuO}_{2.5}$  (in the case of the binary oxide,  $\text{Y}_2\text{O}_3$  was used as received). The heated mixtures were then powdered. The powdered or pelletized starting melting material ( $\text{BaCu}_3\text{O}_4$ ,  $\text{Ba}_2\text{Cu}_3\text{O}_5$  or  $\text{TbBa}_2\text{Cu}_3\text{O}_{6.5+x}$ ) was then placed on the powdered or pelletized solid material (nonstoichiometric Y-Ba-Cu-oxide), heated in flowing oxygen at 950 °C for 24 h in a tube furnace, and then at 650 °C for 4 h. Finally, the materials were fur-

nace-cooled in flowing oxygen to less than 200 °C for 1 to 2 h before they were removed from the furnace.

Upon removal from the furnace the resulting material was found to contain both melted and nonmelted regions. Where the melting starting material (Ba-Cu-O or Tb-Ba-Cu-O) reacted with the nonmelting starting material, a black melt-crystallized superconducting region was formed. This typically took the shape of a hemisphere of about 1 cm in diameter surrounded by the green (nonmelting) phase. The green nonmelted portions were then removed and samples of rectangular parallelepiped geometry were cut with a saw to typical dimensions of  $1 \times 2 \times 7$  mm.

We examine the effect of the melt process on transport critical current and magnetization of the  $\text{YBa}_2\text{Cu}_3\text{O}_{7-x}$  melt sample. X-ray diffraction measurements were carried out using  $\text{CuK}\alpha$  radiation. Standard four-probe resistance measurements were performed using annealed silver paste contacts.<sup>3</sup>

## III. RESULTS

The x-ray data (Fig. 1) show single-phase  $\text{YBa}_2\text{Cu}_3\text{O}_{7-x}$  diffraction patterns for the melt-processed samples with two additional lines [at  $d = 2.52 \text{ \AA}$  ( $\bar{1}11$ ) and  $2.33 \text{ \AA}$  ( $111$ )], characteristic of a small amount of unreacted  $\text{CuO}$  present for both types of melt processing (Ba-Cu-O or Tb-Ba-Cu-O starting compounds). Microprobe analysis show no ( $< 1\%$ ) Tb in the melted portion of the sample in the case of the Tb-based starting compound. Hence, any changes in the transport critical current and magnetization measurements observed between the sintered and melt-processed samples are due to changes in the bulk properties of the material, and we believe that the changes in the bulk properties are a result of the changes in the linking of the superconducting grains. These changes could be caused by

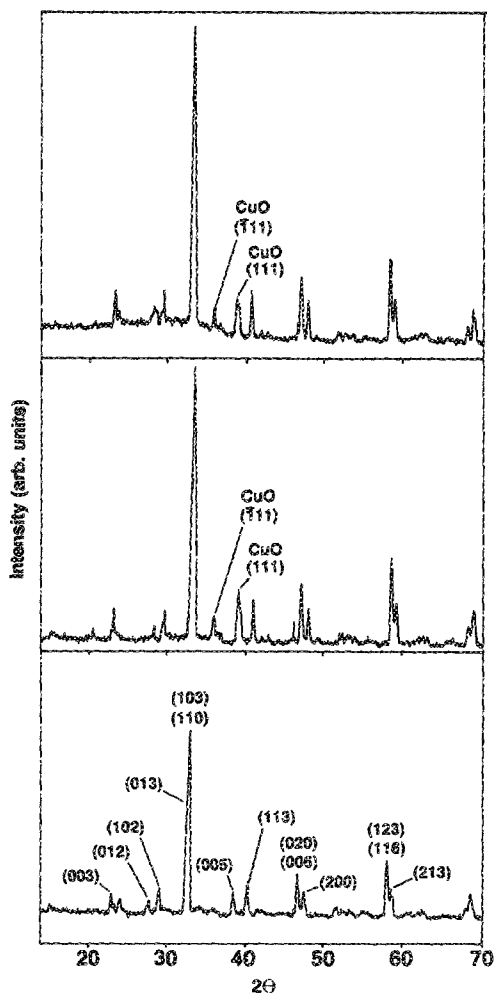


FIG. 1. X-ray powder diffraction data for a sintered  $\text{YBa}_2\text{Cu}_3\text{O}_{7-x}$  (top) and a melt-processed sample (bottom) are compared. The melt-processed sample shows primary single-phase  $\text{YBa}_2\text{Cu}_3\text{O}_{7-x}$  and a small amount of unreacted CuO.

variations in grain overlap, grain size, grain boundary electronic properties, or reduced voids between the grains. Fewer voids are evidenced by an increase in the density of the sample after melt-processing (from 6.1–6.74 g/cm<sup>3</sup>).<sup>2</sup> It has been shown that the ac magnetic susceptibility transition is sharper in the melt-processed samples than that in the sintered samples.<sup>1</sup> A typical resistive transition measured by the standard four-probe technique is shown in Fig. 2.

The critical current measurements presented are those in which the contacts were baked on the sample. The contacts were made with silver paste and the samples were annealed in flowing O<sub>2</sub> at 900 °C, then cooled to room temperature.<sup>3</sup> Wire leads were soldered onto the silver contacts with indium solder. The criterion for the establishment of resistance was the production of 1 μV/mm. In Figs. 3 and 4, we show transport critical current density  $J_c$  as a function of applied magnetic field  $H$  at various temperatures ranging from 4.2 to 77 K. In Fig. 5, the low-field data at 77 K is shown. Also shown (solid line) is a theoretical curve obtained using a Josephson junction grain boundary contact model as discussed in the analysis section. Figure 6 shows the low-field grain decoupling for sample No. 2 at the ratio  $J_c(H)/J_c(0)$  as a function of the applied field.

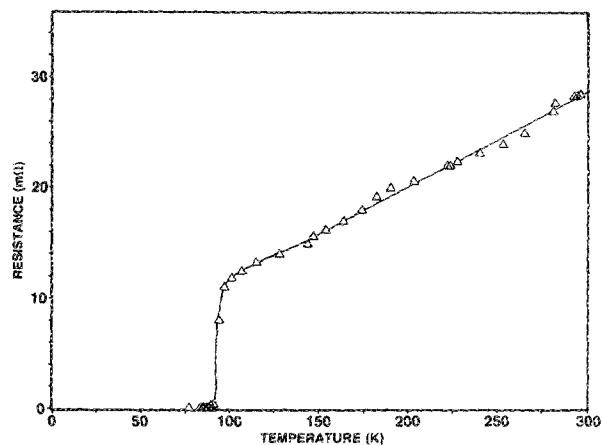


FIG. 2. Resistance as a function of temperature for a Y-Ba-Cu-O sample made by the melt-solid reaction.

Static magnetic susceptibility measurements were made with a SHE variable temperature SQUID susceptometer. The range of temperatures studied was 10–300 K in fields of 0.1 to 10 mT. Two experimental procedures were followed. In the first, the sample was cooled in zero field (ZFC) to 10 K after which the magnetic field was applied. The resulting curve corresponds to the diamagnetic shielding of the sample. In the second, the data were obtained by cooling the sample in constant magnetic field (FC) from room temperature to 10 K. The resulting data correspond to the Meissner effect (or flux expulsion).

We show magnetization data for three samples. One is a conventionally sintered  $\text{YBa}_2\text{Cu}_3\text{O}_{7-x}$  (shown in Fig. 7).

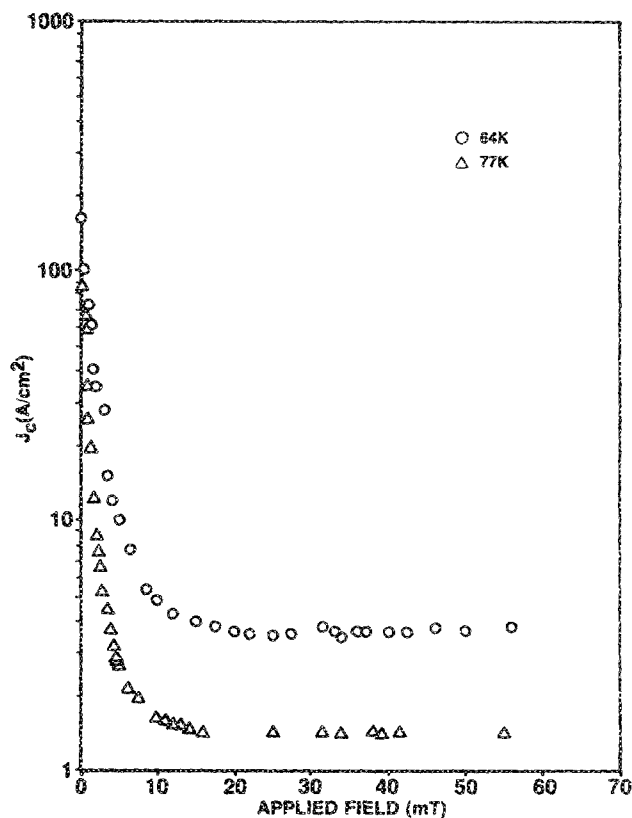


FIG. 3. Critical current as a function of applied magnetic field for melt-processed  $\text{YBa}_2\text{Cu}_3\text{O}_{7-x}$  (sample No. 1).

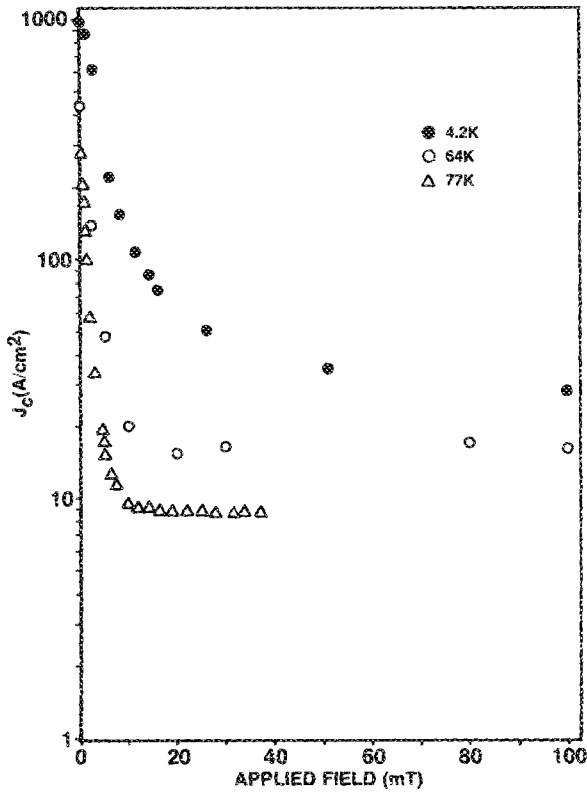


FIG. 4. Critical current as function of applied magnetic field for melt-processed  $\text{YBa}_2\text{Cu}_3\text{O}_{7-x}$  (sample No. 2).

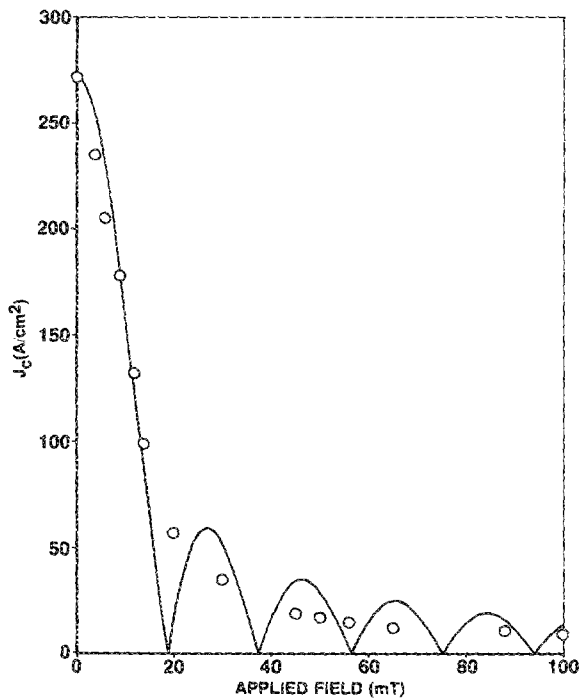


FIG. 5. Theoretical curve (solid line) of the critical current in a single Josephson junction in parallel magnetic field and experimental transport critical current data points for a melt-processed (sample No. 2)  $\text{YBa}_2\text{Cu}_3\text{O}_{7-x}$  at 77 K.

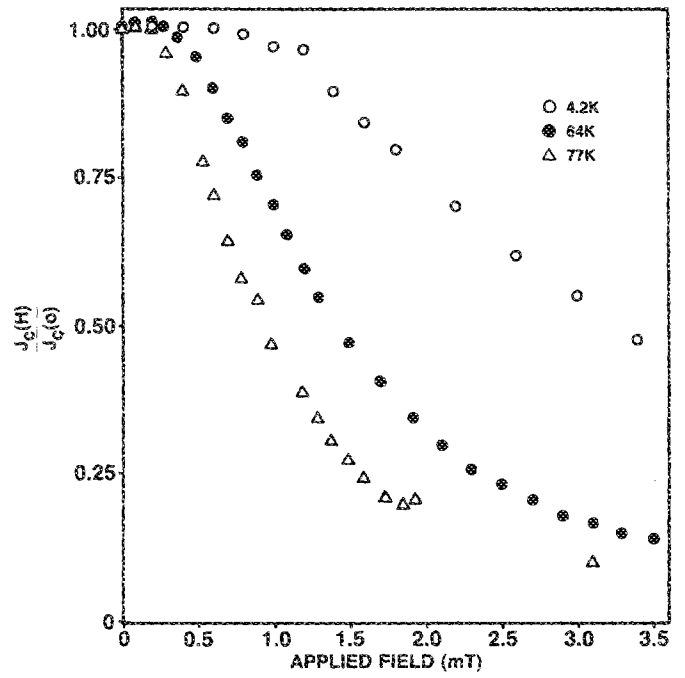


FIG. 6.  $J_c(H)/J_c(0)$  as a function of applied magnetic field at 77, 64, and 4.2 K for a melt-processed (sample No. 2)  $\text{YBa}_2\text{Cu}_3\text{O}_{7-x}$ .

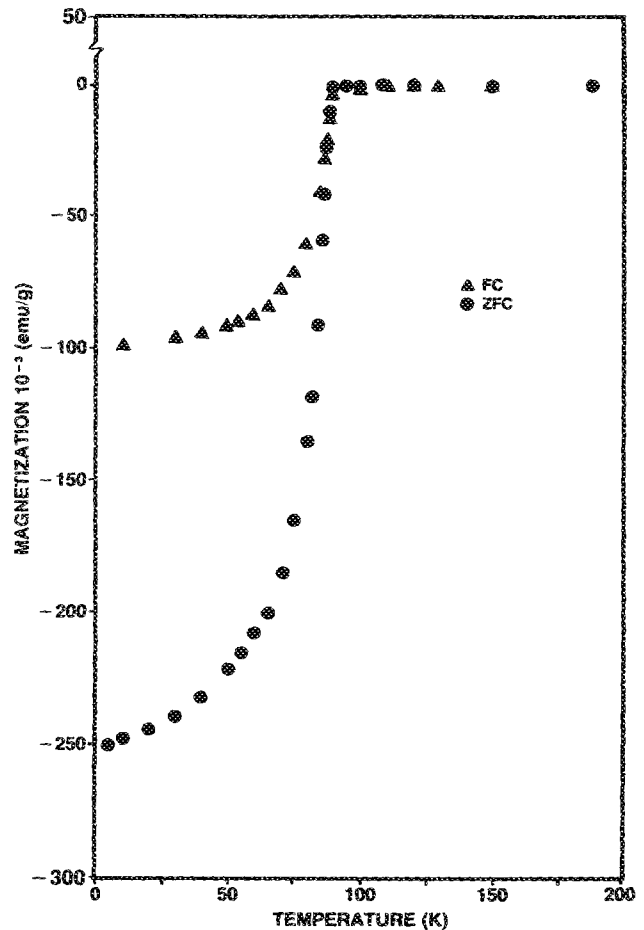


FIG. 7. Magnetization of sintered  $\text{YBa}_2\text{Cu}_3\text{O}_{7-x}$  in an applied field of 1.5 mT. Triangles denote field-cooled data (FC) while circles denote zero-field cooled data (ZFC). Both sets of data were taken during warm up.

The second sample is  $Y_{1.2}Ba_{0.8}CuO_{4-x}$  (green) sample with a resistance above 30 M $\Omega$ , but it shows a strong Meissner effect (shown in Fig. 8). This indicates that the sample has superconducting regions although it does not have a conducting path through the volume of the sample. This sample has the same stoichiometry as the bottom reactant in one of the melt processes. The third sample we studied is a melt-processed superconductor with stoichiometry  $YBa_2Cu_3O_{7-x}$ . Figures 9, 10, and 11 show the magnetization versus temperature for a melt-processed sample in an applied field of 0.1, 1.5, and 10 mT, respectively.

#### IV. ANALYSIS

Following Kwak *et al.*<sup>4</sup> we have modeled the intra-grain connections as a network of Josephson junctions with the junctions randomly oriented with respect to the external field.

Josephson junctions are extremely sensitive to applied magnetic fields and can decouple in fields as small as the earth's field. The current for a square junction of width  $L$  in an applied magnetic field normal to the junction can be expressed<sup>4,5</sup> as

$$I = J_1 \left[ \frac{\sin\left(\frac{\pi\theta}{\theta_0}\right)}{\left(\frac{\pi\theta}{\theta_0}\right)} \right],$$

where  $\theta = HL(2\lambda + 1)$  and  $\theta_0 = hc/2e$ ,  $H$  is the applied magnetic field parallel to the planar faces of the junction,  $\lambda$  is the penetration depth,  $l$  is the separation of the junction

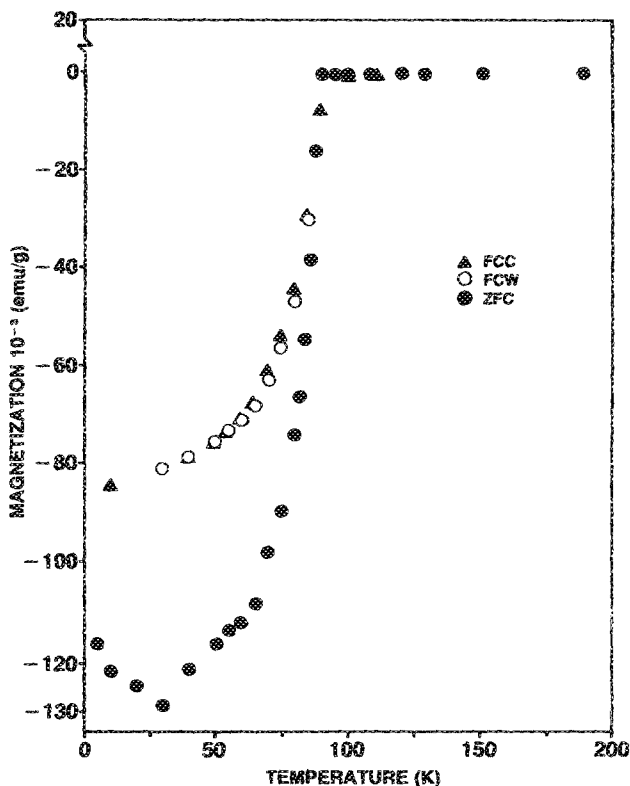


FIG. 8. Magnetization of sintered  $Y_{1.2}Ba_{0.8}Cu_3O_{7-x}$  in an applied field of 1.5 mT. Triangles denote field cooled data taken during cool down (FCC), while open circles denote field-cooled data taken during warm up (FCW). Darkened circles denote data taken with zero-field cooling during warm up (ZFC).

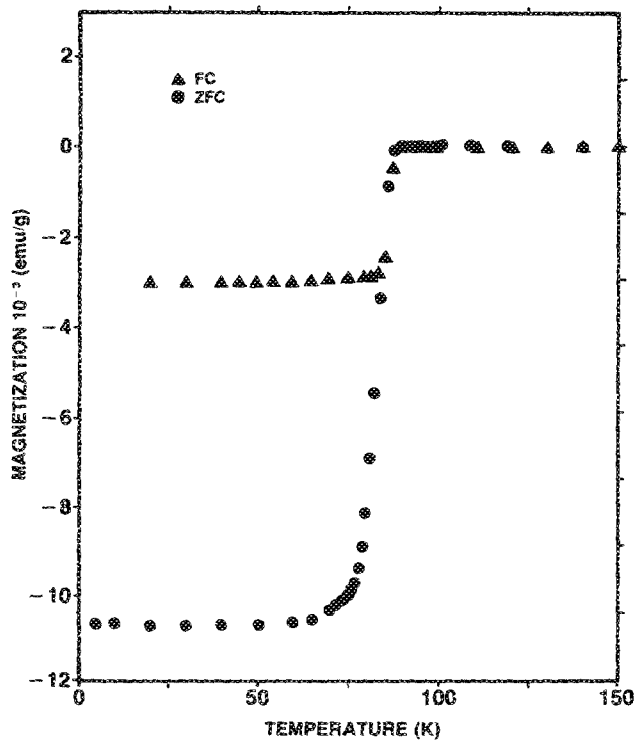


FIG. 9. Magnetization of melt-process  $YBa_2Cu_3O_{7-x}$  in an applied field of 0.1 mT. Triangles denote field-cooled data (FC) while circles denote zero-field-cooled data (ZFC). Both sets of data were taken during warm up.

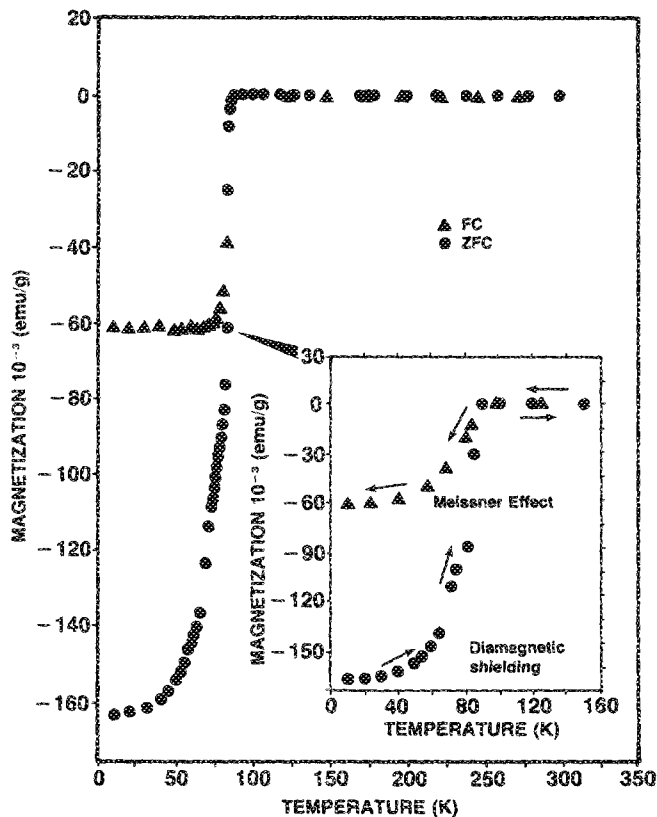


FIG. 10. Magnetization of melt-processed  $YBa_2Cu_3O_{7-x}$  in an applied field of 1.5 mT. Triangles denote field-cooled data (FC) while circles denote zero-field-cooled data (ZFC). Both sets of data were taken during warm up.

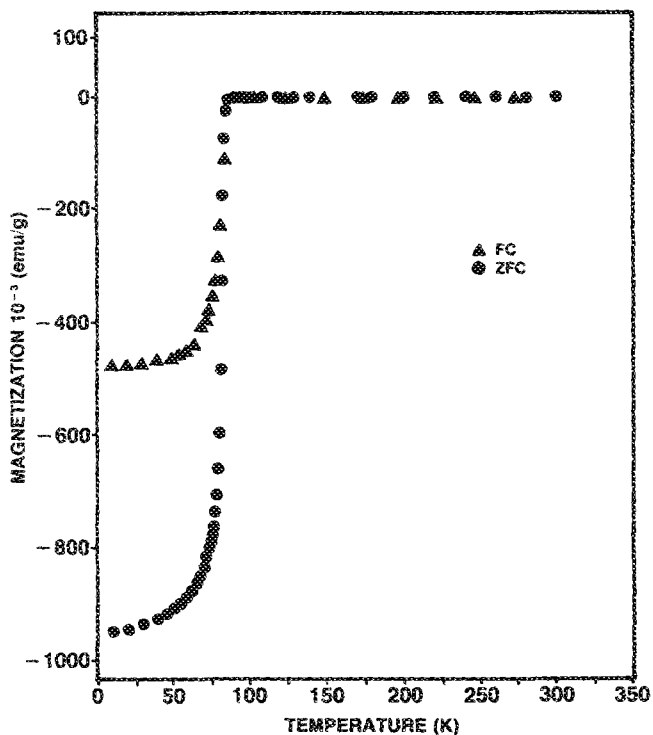


FIG. 11. Magnetization of melt-processed  $\text{YBa}_2\text{Cu}_3\text{O}_{7-x}$  in an applied field of 10 mT. Triangles denote field-cooled data (FC) while circles denote zero-field-cooled data (ZFC). Both sets of data were taken during warm up.

faces, and  $J_j$  is the zero-field critical current density of the junction times the junction area ( $L^2$ ).

In Fig. 5, we show a plot of the above equation for  $H$  ranging from 0 to 10 mT.  $J_j$  is determined from our experimental data from sample No. 2. We have used  $2L\lambda$  equal to  $1.1 \times 10^{-10} \text{ cm}^2$  to obtain the best-fit curve. If grain decoupling is occurring in the sample, we expect a rapid drop in the transport critical current as the magnetic field is increased (which we observe).

Our data reflects the qualitative behavior of the model (i.e., rapid decoupling) but not the details of the interference pattern. This is explained by the grain boundaries acting as Josephson junctions distributed with random orientations with respect to the external field. These combine to wash out the details of the interference pattern.

The effect of the decoupling is shown by the fact that  $J_c$  has decreased to approximately 10% of the zero-field value ( $84 \text{ A/cm}^2$  to  $8 \text{ A/cm}^2$ ) by  $H = 2 \text{ mT}$  for sample No. 1. Above  $H = 10 \text{ mT}$ ,  $J_c$  decreases very slowly.

The zero-field critical current values are about  $200 \text{ A/cm}^2$  with a large variation between samples, as is apparent from Figs. 3 and 4 with sample No. 1 having a value of  $84 \text{ A/cm}^2$  at  $77 \text{ K}$  and sample No. 2 having a value of  $272 \text{ A/cm}^2$  at  $77 \text{ K}$ . These zero-field critical current values are comparable to those of the best conventionally prepared untextured sintered materials. These figures also show a rapid decrease of the transport critical current in the presence of weak magnetic fields. Sample No. 2 shows considerable decoupling but not as great as in sample No. 1 with the  $J_c(H)$  decreasing by 75% at  $2 \text{ mT}$  at  $77 \text{ K}$ .

Using the density of the sintered  $\text{YBa}_2\text{Cu}_3\text{O}_{7-x}$  ( $6.1 \text{ g/cm}^3$ ) and correcting for the demagnetization effect for the sample geometry we obtained  $-4\pi\chi = 0.85$  (from ZFC data) at  $1.5 \text{ mT}$ . This implies that at this field the coupled grains almost completely exclude the flux from the sample interior.

The ZFC data for the  $\text{Y}_{1.2}\text{Ba}_{0.8}\text{CuO}_{4-x}$  material are systematically smaller in superconducting volume fraction than those for the sintered  $\text{YBa}_2\text{Cu}_3\text{O}_{7-x}$ . This fact indicates that in the green material the grains are decoupled or separated by insulating boundaries. We believe that this is the reason why the sample shows levitation but no conduction. Therefore the ZFC data, for this particular material, reflect the screening of the field by the individual grains. The FC data reflect the expulsion (and trapping) of the field by the grains. Hence, the difference between these two sets of data is a measure of the flux trapped at the pinning centers.

To obtain an estimate of the volume fraction of superconducting phase, we take the ratio of the field-cooled magnetization and the zero-field cooled magnetization ( $M_{FC}/M_{ZFC}$ ) at a temperature below the critical temperature. This ratio gives approximately one third of the sample as superconducting. For the melt-processed sample in an applied magnetic field equal to  $0.1$  or  $1.5 \text{ mT}$ , the ratio of  $M_{FC}/M_{ZFC}$  shows that approximately one third of the volume is superconducting. However, for  $H$  equal to  $10 \text{ mT}$ , approximately half of the volume is superconducting. The ratio of  $M_{FC}/M_{ZFC}$  is depressed with increasing magnetic field. This latter feature is taken as a further indication of grain decoupling at higher field which reduces the (absolute) value of the ZFC signal. Several papers have shown<sup>4,6</sup> that for sintered samples, many of the grains have decoupled at fields as low as  $1.5$  to  $2 \text{ mT}$ . However, in the melt sample, the SQUID data indicate that the decoupling is not perfect below  $10 \text{ mT}$ . This is also consistent with the observed non-zero  $J_c$  in this range of magnetic field, as could be seen in Figs. 3 and 4.

Both shielding and flux expulsion of the melt-processed samples were observed to be approximately temperature independent below  $60 \text{ K}$  indicating strong coupling between the grains, or effective superconducting shorts between grains throughout the entire volume below this temperature. The volume fraction of superconducting material in the melt-processed sample is slightly lower than in the sintered sample, but the transition is sharper.

## V. SUMMARY

We have measured the transport critical current for melt-processed  $\text{YBa}_2\text{Cu}_3\text{O}_{7-x}$  and showed that it is comparable to the best of the conventionally prepared sintered samples.<sup>6</sup> Magnetization data were presented for melt-processed and sintered samples. Both shielding and flux expulsion of the melt-processed samples were observed to be approximately temperature independent below  $60 \text{ K}$  indicating superconducting shorts between the grains throughout the entire volume below this temperature. The behavior of  $J_c$  in a magnetic field can be explained using a model of weakly-linked superconducting regions. The ZFC

magnetization is depressed with high applied magnetic fields which is also indicative of grain decoupling.

#### ACKNOWLEDGMENTS

The work at Cleveland State University was supported by the National Aeronautics and Space Administration Grants Nos. NCC-3-19 and NAG-3-873. The authors wish to thank D. Liebal and J. Marino for technical assistance.

<sup>1</sup>A. M. Hermann, Z. Z. Sheng, W. Kiehl, D. Marsh, F. Arammash, A. El Ali, D. Mooney, L. Sheng, J. A. Woollam, and A. Ahmed, *Appl. Phys. Commun.* **7**, 275 (1987).

<sup>2</sup>A. M. Hermann and Z. Z. Sheng, *Appl. Phys. Lett.* **51**, 1854 (1987).

<sup>3</sup>J. Van Der Mass, V. A. Gasparov, and D. Pavana, *Nature (London)* **328**, 603 (1987).

<sup>4</sup>J. F. Kwak, E. L. Venturini, D. S. Ginley, and W. Fu, in *Novel Superconductivity*, edited by S. A. Wolf and V. Z. Kresin (Plenum, New York, 1987), p. 983.

<sup>5</sup>C. B. Duke, *Tunneling in Solids* (Academic, New York, 1969).

<sup>6</sup>J. W. Ekin, *Adv. Ceramic Mater.* **2**, 586 (1987).